Protein Engineering, Design & Selection vol. 18 no. 5 pp. 221–228, 2005
Published online April 8, 2005 doi:10.1093/protein/gzi024

Homology modelling of transferrin-binding protein A from *Neisseria meningitidis*

Jonathan S.Oakhill[1,2], Brian J.Sutton[1], Andrew R.Gorringe[3] and Robert W.Evans[1,4]

[1]Metalloprotein Research Group, Randall Division of Cell and Molecular Biophysics, King's College London, New Hunt's House, Guy's Campus, London SE1 1UL and [3]Health Protection Agency, Salisbury SP4 0JG, UK

[2]Present address: Division of Life Sciences, King's College London, Franklin-Wilkins Building, Waterloo, London SE1 9NH, UK

[4]To whom correspondence should be addressed.
E-mail: robert.evans@kcl.ac.uk.

***Neisseria meningitidis*, a causative agent of bacterial meningitis, obtains transferrin-bound iron by expressing two outer membrane located transferrin-binding proteins, TbpA and TbpB. TbpA is thought to be an integral outer membrane pore that facilitates iron uptake. Evidence suggests that TbpA is a useful antigen for inclusion in a vaccine effective against meningococcal disease, hence the identification of regions involved in ligand binding is of paramount importance to design strategies to block uptake of iron. The protein shares sequence and functional similarities to the *Escherichia coli* siderophore receptors FepA and FhuA, whose structures have been determined. These receptors are composed of two domains, a 22-stranded β-barrel and an N-terminal plug region that sits within the barrel and occludes the transmembrane pore. A three-dimensional TbpA model was constructed using FepA and FhuA structural templates, hydrophobicity analysis and homology modelling. TbpA was found to possess a similar architecture to the siderophore receptors. In addition to providing insights into the highly immunogenic nature of TbpA and allowing the prediction of potentially important ligand-binding epitopes, the model also reveals a narrow channel through its entire length. The relevance of this channel and the spatial arrangement of external loops, to the mechanism of iron translocation employed by TbpA is discussed.**

Keywords: iron/meningococcal/TbpA/transferrin

Introduction

Iron acquisition is a particular problem for pathogenic bacteria owing to the low levels found within the human host. Most body iron is inaccessible, being complexed to haemoglobin or stored in ferritin, and bacteriostatic conditions are further maintained by the rapid sequestering of free iron by glycoproteins such as human transferrin (hTf), found in the blood plasma and human lactoferrin (hLf), found on mucosal surfaces and in secretions. Microbes have therefore evolved a number of different mechanisms to survive in this iron-restricted environment. Many bacteria are capable of secreting siderophores, low molecular weight molecules that are extremely effective iron chelators in the local environment (Griffiths and Williams, 1999). These scavenging molecules compete for iron with host iron-binding proteins before re-uptake by specific, integral outer membrane receptors. *Escherichia coli* secretes a variety of siderophores, including enterobactin and ferrichrome, whose internalization into the periplasm is mediated by their specific receptors FepA and FhuA, respectively.

Some bacteria such as *Neisseria meningitidis*, a causative agent of bacterial meningitis and septicaemia, are able to interact directly with host iron-glycoproteins, stripping iron from their binding sites for translocation across the outer membrane. Binding and mutational studies (Schryvers and Lee, 1989; Blanton *et al*., 1990) showed that in *Neisseria*, iron uptake from hTf and hLf occurs via two distinct but parallel pathways. Utilization of either hTf or hLf as sources of iron requires specific receptors that are exposed at the cell surface. Iron uptake from hTf is mediated by a complex of two transferrin-binding proteins (TbpA and TbpB), whereas lactoferrin-binding protein complexes are associated with iron uptake from hLf. TbpA has a molecular weight of ∼98 kDa and displays a high degree of sequence homology between strains (Pajón *et al*., 1997). It is thought to exist as an integral outer membrane protein, through which iron is transported into the periplasmic space (Gorringe and Oakhill, 2002). TbpA is currently being considered as a candidate for inclusion in a meningococcal vaccine effective against all serogroups. Recombinant TbpA produces a strong immunogenic response in mice, protecting them from subsequent intraperitoneal challenge with *N.meningitidis* (West *et al*., 2001), while antibodies in sera from diseased patients cross-react with a range of meningococcal isolates (Gorringe *et al*., 1995; Johnson *et al*., 1997). TbpB displays greater sequence heterogeneity between strains and ranges in molecular weight from 65 to 85 kDa. It is thought to be fully surface exposed, attached to the outer membrane via an N-terminal lipid moiety (Gerlach *et al*., 1992) and acts as an accessory protein to TbpA by increasing the affinity of the Tbp complex for iron-loaded hTF.

Despite the variation in the nature of the initial iron-chelated complex that is presented to all of these uptake pathways, it is clear that these iron-uptake receptors share remarkable structural and functional similarities. Iron translocation is reliant on a proton-motive force generated at the inner membrane and passed across the periplasm via the transducer protein TonB (Bradbeer, 1993). The identification of a conserved, TonB-interacting pentapeptide sequence at the N-termini of these receptors classifies TbpA, FepA, FhuA and the diferricitrate receptor FecA into the family of TonB-dependent proteins. The crystal structures of FepA (Buchanan *et al*., 1999), FhuA (Ferguson *et al*., 1998; Locher *et al*., 1998) and FecA (Ferguson *et al*., 2002) have shown that each is composed of a 22-stranded anti-parallel β-barrel spanning the outer membrane, connected via a short hinge region to an N-terminal plug domain which folds into the barrel, being held in place by numerous hydrogen bonds and polar contacts. These plug domains possess a structurally conserved core formed mainly

by a mixed four-stranded β-sheet tilted at a 45° angle to the barrel axis, an orientation which physically separates the ligand binding pocket on the extracellular surface of the receptor from a smaller pocket exposed to the periplasm. The external binding site is also bordered by surface-exposed residues within plug domain loops (two in FepA, three in FhuA and FecA) that extend above the β-sheet core.

The significance of these loops is not clear, although their close proximity to the binding pocket and the fact that they possess stretches of high sequence variation between the three receptors suggests they play a role in ligand recognition. Comparisons between the structures of FhuA and FhuA–ferrichrome–iron complex (Ferguson *et al.*, 1998) indicate that these loops form the origin of a signal to initiate an interaction with TonB at the periplasmic surface, prior to iron translocation. Upon ferrichrome binding, the apex of one of these loops is translated 1.7 Å towards the ligand. The rearrangement is asymmetrically propagated across the plug domain, resulting in the complete unfolding of a switch helix (residues 24–29) at the periplasmic surface. This causes the TonB box to swing to the opposite side of the barrel, possibly acting as a signal to initiate the selective binding of TonB. Opinion is divided on the sequence of events that follow to allow iron uptake (Faraldo-Gómez and Sansom, 2003): either the plug domain unfolds to some extent and is ejected from the barrel to uncover a pore large enough for siderophore transport (Usher *et al.*, 2001) or the structural rearrangement following ligand binding is itself sufficient to open a channel of adequate size, as seen in the FhuA–ferrichrome–iron complex.

Size constraints prevent hTf from passing through the TbpA β-barrel, hence the mechanism employed by the Tbps would require additional steps to remove iron at the external surface of the receptor. It has previously been speculated that binding of external loops of the TbpA β-barrel to hTf, followed by a succession of conformational changes, could forcibly separate the domains surrounding the iron-binding site. The concomitant reduction in affinity of hTf for iron would then cause the ferric ion to be released directly into the TbpA pore (Boulton *et al.*, 1999; Schryvers and Stojiljkovic, 1999). Allosteric changes within the β-barrel domain of TonB-dependent proteins upon ligand binding have been observed previously, most notably in comparisons of the structures of FecA and FecA–diferricitrate complex (Ferguson *et al.*, 2002). Formation of the liganded complex causes a major spatial rearrangement of external loops 7 and 8, with a maximum displacement of up to 15 Å, that seals off the binding pocket from the extracellular environment. This suggests that the β-barrel domain itself, perhaps utilizing energy provided by TonB, plays an active role in iron uptake.

The structural homology displayed by the TonB-dependent receptors permits modelling of the 3D structure of TbpA in the absence of crystallographic data. Any structural information regarding TbpA would be extremely beneficial for the development of an effective multi-serogroup vaccine, particularly if inferences can be made as to the location of putative hTF-binding domains. Antibodies specifically designed to recognize these epitopes would not only target the pathogen for opsonisation, but also deny it a valuable iron source. A 3D model for meningococcal TbpA, based on the structures of FepA and FhuA–ferrichrome complex, has been developed for this purpose and is described here.

Materials and methods

2D topology modelling

The solved structure files for FepA (1fep) and FhuA–ferrichrome complex (1by5) were obtained from the PDB database. The sequence of TbpA from *N.meningitidis*, strain K454 (B15:P1:7,16), was retrieved from the TrEMBL database (AC: Q9JPJ0). Initial steps to determine a 2D TbpA topology model focused on identifying short hydrophobic regions (7–11 residues) within the sequence that might traverse the lipid bilayer and form the β-barrel. Although many computer-based algorithms are able to predict regions of elevated hydrophobicity within a sequence, most do not take into account the particular hydrophobic environment found within a transmembrane β-barrel. Only one side of a β-sheet within a membrane buried sequence is required to display any degree of hydrophobic character, since only alternate (i.e. externally oriented) residues are in contact with the lipid bilayer.

This criterion is accounted for by the prediction program of Schirmer and Cowan (1993), which assigns an average hydrophobicity value (H_s) to each residue based on a hydrophobicity index (Eisenberg *et al.*, 1984). The algorithm was initially tested with the FepA and FhuA β-barrel sequences, and, once parameters for assigning transmembrane domains had been optimized provided the most accurate topology predictions compared with other web-based programs tested. Twenty-two highly probable transmembrane strands were selected for TbpA, starting from the C-terminus, which was assigned as being located within the periplasm as for FepA and FhuA.

In silico 3D structure modelling

The β-barrel backbone of the 3D TbpA model was constructed based on the β-barrel portion of the 2D TbpA model. This sequence was manually aligned with the sequence of the FhuA β-barrel such that the 22 putative TbpA transmembrane strands corresponded to those of FhuA. Insertions found in the external loops of the 2D TbpA model that were absent from the FhuA structure were removed from the alignment. The program Modeller 4 (Sali and Blundell, 1993) used this alignment and the structure of the FhuA β-barrel to appoint coordinates to atoms constituting the TbpA protein backbone. This allowed the construction of the TbpA β-barrel backbone from a single alignment, with the advantage that each TbpA transmembrane strand was automatically oriented with regard to its neighbour. Side-chain conformations were then determined based on the predicted secondary structure of the protein sequence of the β-barrel backbone.

Conformations of the TbpA external loops omitted from the initial alignment were then calculated, using templates obtained from the program 3D-PSSM (Kelley *et al.*, 2000). This searches databases of known 3D structures with sequence homology to the target sequence. Templates were selected for each TbpA insert, based on visual assessment and the avoidance of bad steric interactions. Side-chain conformations in these loops were assigned using Homology (Greer, 1990). Finally, these external loop regions were spliced on to the TbpA β-barrel backbone using GENLOOP, to construct the entire TbpA β-barrel.

The 3D structure of the putative N-terminal plug domain was determined using the structure of the FepA plug domain as a template. A multiple sequence alignment between the

150 residues following the TonB boxes of TbpA, FepA and 12 other TonB-dependent proteins was compiled by ClustalX, in this case to predict more accurately regions of conserved secondary structure. The alignment between TbpA and FepA was extracted from this, which Modeller 4 used to construct the protein backbone of the TbpA plug domain. Side-chain conformations in this domain were again assigned using Homology.

Both the plug and β-barrel domains of TbpA were then superimposed on that of the entire FhuA structure using Homology, with the TbpA and FhuA plug domains oriented such that the four-stranded β-sheet cores were superimposed. This orientation involved minimizing bad steric interactions with the inner TbpA barrel surface, while maximizing hydrogen bond interactions between residues conserved in both TbpA and FhuA. The two TbpA model portions were joined together at the hinge region using GENLOOP to complete the initial 3D model.

3D model refinement

Energy minimization was performed using the molecular dynamics program CHARMM (Brooks *et al*., 1983). The stereochemical quality of the 3D model was assessed throughout the minimization procedure using PROCHECK (Laskowski *et al*., 1993).

Results

The topology program used to predict the 2D TbpA model produces a graph displaying the H_s value of each residue (not shown), with peaks indicating regions of elevated hydrophobicity. An H_s value of +0.75 was found to be optimal for the prediction of FepA and FhuA transmembrane strands, above which the residue and neighbouring sequence were deemed to be embedded within the lipid bilayer. In the case of both FepA and FhuA, this threshold value correctly assigned 19 of the 22 transmembrane strands without any false-positive predictions. Since the periplasmic loops of both proteins are short, H_s peaks were assumed to occur in 'pairs' within the graph, allowing the simple assignation of the remaining three transmembrane strands. When applied to the TbpA sequence and using the same threshold H_s value, the topology prediction program assigned 18 peaks as representing transmembrane strands. Smaller peaks adjacent to four unpaired peaks in the graph were assigned as the remaining four strands.

Clues concerning the precise location of transmembrane strands come from the membrane interfaces. The first high-resolution porin structures (Weiss *et al*., 1991; Schirmer *et al*., 1995; Meyer *et al*., 1997) indicated that regions of membrane proteins located at these interfaces are enriched in particular amino acids. Membrane interfaces were often delineated by polar-aromatic residues (tryptophan and tyrosine) that formed two belts around the external surface of the β-barrel, from where they could interact favourably with lipid headgroups in the membrane. This pattern of polar-aromatic localization is also evident in the structures of FepA, FhuA and FecA and is thought to increase barrel stability. Assignment of transmembrane sequences within the TbpA model was altered to maximize the number of these stabilizing residues present.

The 2D TbpA topology model is shown in Figure 1a. In the membrane, the first transmembrane strand would form hydrogen bonds with the last transmembrane strand to form the β-barrel. The model possesses a 158 residue N-terminal plug domain that would sit within the 22-stranded β-barrel, with β-strands ranging in length from 10 to 20 residues. The external loops range in length from 4 (loop 1) to 85 (loop 2) residues, while none of the periplasmic loops exceed six residues. Six cysteine residues are located in external loops and may contribute to the formation of a disulphide bond in each of loops 2, 4 and 5. The model also possesses two continuous girdles of aromatic residues delineating the upper and lower boundaries of the membrane.

This topology model, along with a sequence alignment of the putative barrel portion of TbpA and the FhuA β-barrel, was used as a basis for the construction of a 3D model. The alignment was manually altered as described in the Materials and methods section and the two sequences were found to share an identity of 10.5% and a similarity of 24.4%. However, the TbpA sequence contains several large insertions that are proposed to be located within all of the predicted external loops, except for loops 1, 6 and 9. With these insertions removed, the sequences of the TbpA and FhuA β-barrel domains share 14.3% identity and 32.3% similarity (the alignment of which is shown in Figure 2). The β-barrel domains of FepA and TbpA share a sequence identity of 6.7% and a similarity of 22.1% when aligned in a similar manner, hence FhuA was selected as the template for the 3D TbpA β-barrel model. TbpA peptides removed from the TbpA/FhuA alignment were used to search the 3D PSSM database, the results of which are shown in Table I.

The N-terminal 150 residues following the TonB box of TbpA were aligned with the sequences from 13 TonB-dependent proteins. The alignment indicates the presence of 'homology islands', short stretches of residues that are either identical or possess conserved character between each sequence. Figure 3 shows this alignment between TbpA and FepA only. The residues that contribute to the six β-sheets and two sensor loops of the FepA plug are indicated. The homology islands evident in the alignment appear to be primarily located within these β-sheet structures, while non-conserved residues, insertions or deletions align within the external facing loops of FepA. The sequences share an identity of 19.4% and a similarity of 34.8%, while the plug domains of FhuA and TbpA share a sequence identity and similarity of only 15.2 and 27.9%, respectively. The alignment with the FepA plug domain was therefore used by Modeller 4 to construct the plug domain of TbpA, which was spatially oriented within the β-barrel domain using Homology. Manual alteration of problematic ϕ/ψ angles along the entire protein backbone was performed during the refinement phase of the model construction. After refinement, bump checks revealed that no atom centres were closer than 0.95 Å to each other.

Figure 1b and c show ribbon diagrams of the final 3D model in which the putative N-terminal domain is clearly located within a 22-stranded β-barrel. After structural validation, the TbpA model has been deposited in the PDB (accession code: 1Z2Y). The model possesses a total height of 92 Å and an ellipsoidal cross-section of 56 × 38 Å. When the model is viewed from the periplasmic surface along the barrel axis, the plug domain appears to occlude the transmembrane pore completely, as with FepA and FhuA. The TonB box is evident at the internal surface of the protein and is predicted to extend up to 15 Å into the periplasm. In the model, each transmembrane β-strand is connected by 12 external loops, the longest of

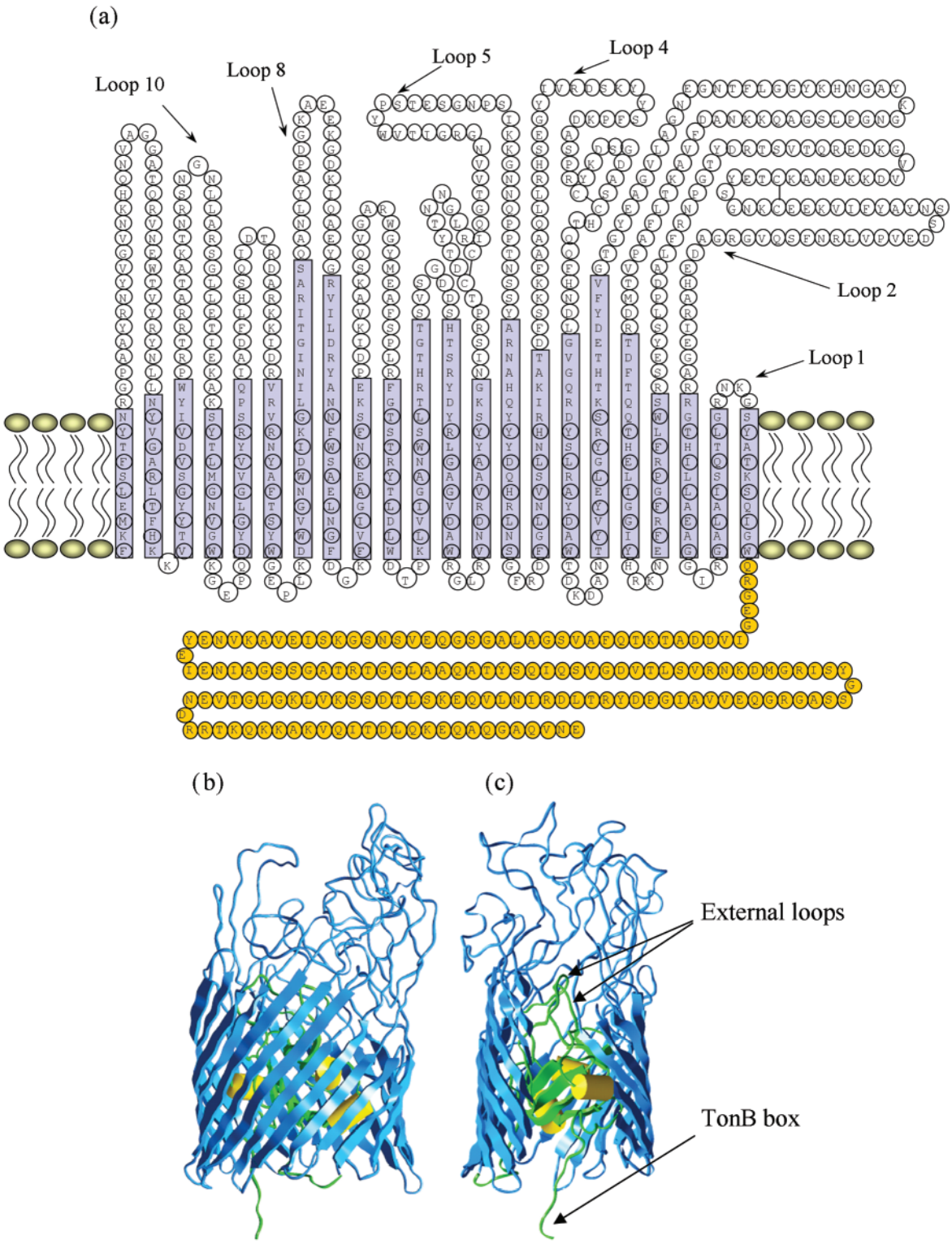

Fig. 1. (**a**) Topology model of meningococcal TbpA, strain K454. The plug region is shaded in orange, while β-strands are shaded in blue. Potential disulphide bonds are indicated by black lines. β-Strand residues with side chains pointing into the hydrophobic environment of the lipid bilayer are shown in bold circles. (**b**), (**c**) Ribbon diagram of the 3D TbpA model. The β-barrel is shown in blue, while the plug region is coloured green. α-Helices within the plug are coloured yellow. Image (c) is oriented 90° along the barrel axis to (b) and the front portion of the barrel has been removed for clarity.

which, loop 2, is made up of 85 residues and extends into the external milieu by >60 Å. Given some flexibility in the loops and the degree of confidence with which they can be modelled, localized structure allows the formation of the three disulphide bonds highlighted in the topology model. Sulphur atoms from C228 and C236 in loop 2, C410 and C419 in loop 4 and C526 and C536 in loop 5 are 4.8, 2.5 and 4.1 Å apart, respectively. The disulphide bond in loop 5 causes the protein backbone to fold back on itself and run along the outside of the external rim of the β-barrel, rather than extend away from the membrane.

A large cleft is seen at the external surface of the receptor, bordered on one side by loops 2, 3 and 4 and on the other by loops 7, 8 and 9. In this static model, surface exposure of the plug domain is restricted by external loops 2, 3 and particularly 4 to a channel ~15 Å in diameter. Siderophore access to the FepA and FhuA plug domains occurs through larger channels (~20 Å in diameter) since external loops 2, 3 and 4 are much shorter in these proteins. When viewed in the same orientation, the TbpA model possesses 26 hydrophilic charged, surface exposed residues that have the potential to interact with hTf, 16 of which are positively charged. FepA and FhuA only possess 14 and 15 surface-exposed, charged residues respectively, with a bias toward negatively charged side chains. This suggests an additional function for the long external loops of TbpA, rather than just acting to form a barrier to solutes during iron translocation. Two loops extend from the external surface of the TbpA plug domain, each of which contains an arginine residue (R57 and R96) that may be important for ligand recognition.

A particular concern in the TbpA modelling process was the correct orientation of the plug domain within the β-barrel, given that the two domains were constructed independently. This was aided substantially by a high degree of secondary structure conservation between the plug domains of model and template; the domain in the TbpA model possessed a four-stranded mixed β-sheet that was virtually superimposable on that of the FepA plug domain. Residues involved in hydrogen bond interactions between the plug domain and the interior of the barrel wall were also used as reference points to assess the reliability of this orientation step. A structurally conserved cluster of residues that are thought to fix the plug to the β-barrel is evident in FepA and FhuA. This region includes two plug domain arginine residues that are close enough to two β-barrel glutamate residues to enable salt-bridge formation. The sequence alignments used to construct the TbpA model (Figures 2 and 3) show that TbpA retains identical charges at these positions despite sequence variation. If the TbpA plug domain was positioned correctly within the β-barrel, it

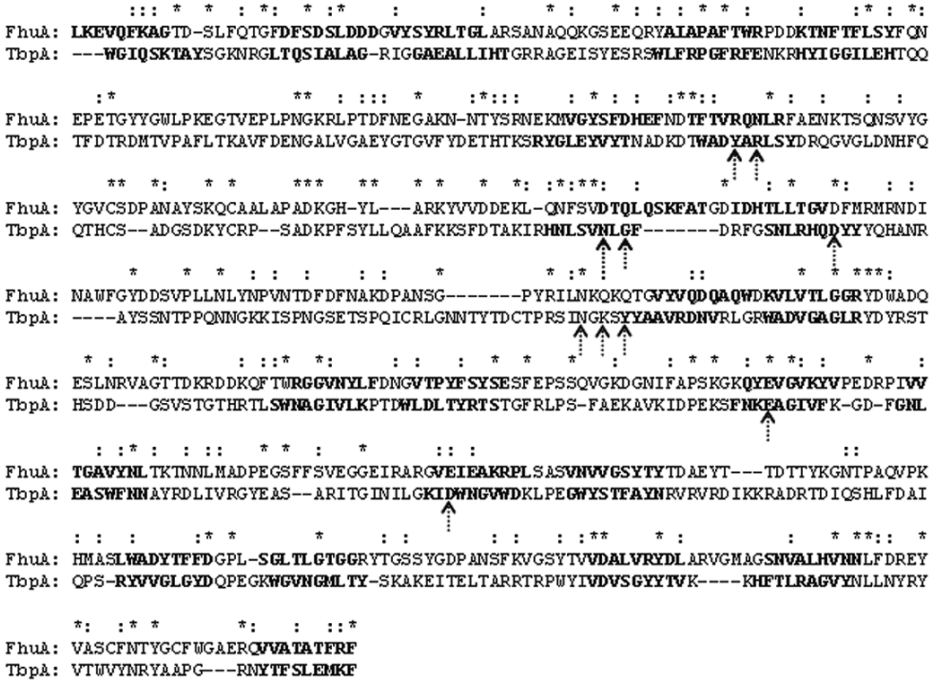

Fig. 2. Sequence alignment of the FhuA β-barrel and the TbpA β-barrel with large insertions removed. Residues constituting transmembrane strands are shown in bold. Asterisk indicates sequence conservation; colon indicates sequence similarity. Solid arrows indicate FhuA residues involved in salt-bridge formation with plug domain residues. Broken arrows indicate FhuA residues lining the putative channel.

Table I. Fragment templates provided by 3D-PSSM for TbpA external loops

TbpA model region	TbpA sequence	Structure template PDB code	Sequence identity (%)
Loop 2	RAHEDAGRGVQSFNRLVPVEDSSN	1b8w (Torres *et al*., 1999)	20.8
Loop 2	YAYFIVKE	1dec (Krezel *et al*., 1994)	12.5
Loop 2	ECKNGSYETCKANPKKGVVGKDERQTVSTRDYT	1esk (Morellet *et al*., 1998)	35.1
Loop 2	GPNRFLADPL	1fep (Buchanan *et al*., 1999)	40.0
Loop 3	ANKKQAGSLPGNGKYAGNHKYGGLFTNG	1xkb (Kamata *et al*., 1998)	17.5
Loop 4	YKSDRVIYGESHR	1zfd (Neuhaus *et al*., 1992)	21.4
Loop 5	YWVTIGRGNVVTG	2fn2 (Sticht *et al*., 1998)	30.7
Loop 7	MYGWRAGVQSKA	1fep	25.0
Loop 8	QIKDGKEEAKGDPAYLNAQ	1pho (Cowan *et al*., 1992)	26.0
Loop 10	LGSRALLNGNSRNTKA	1mgx (Freedman *et al*., 1996)	25.0
Loop 11	ENVRQTAGGAVNQHKNVGV	1fep	15.7

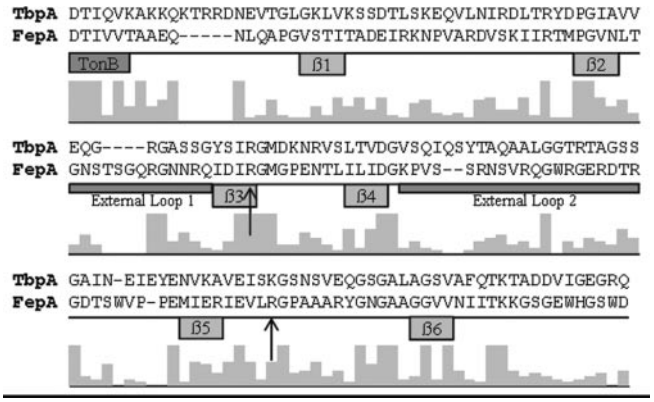

Fig. 3. Sequence alignment of the 150 residues following the TonB box of TbpA and FepA. Grey bars below the alignment indicate the degree of conservation between the sequences as calculated by ClustalX. Residues comprising β-sheet structures within the FepA plug domain are indicated, as are the two external facing loops. Arrows indicate residues involved in salt-bridge formation with barrel residues.

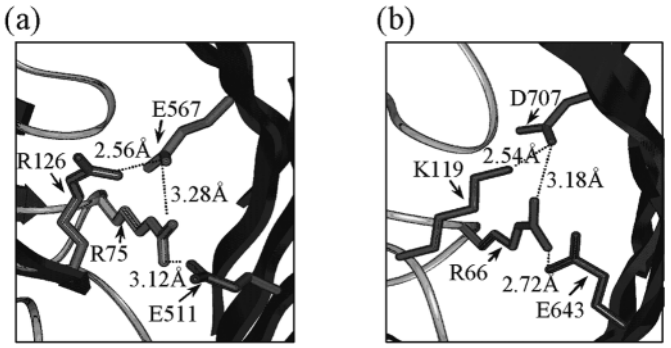

Fig. 4. Salt-bridge formation between plug and barrel residues of FepA (**a**) and the TbpA model (**b**). β-Barrels of FepA and TbpA are shown in black and the plug domains of both structures are represented as light-grey ribbons. The side chains of residues proposed to form salt bridges are also shown. Distances between the nitrogen atoms of positively charged residues (R75 and R126 in FepA, R66 and K119 in TbpA) and the oxygen atoms of negatively charged residues (E511 and E567 in FepA, E643 and D707 in TbpA) are displayed.

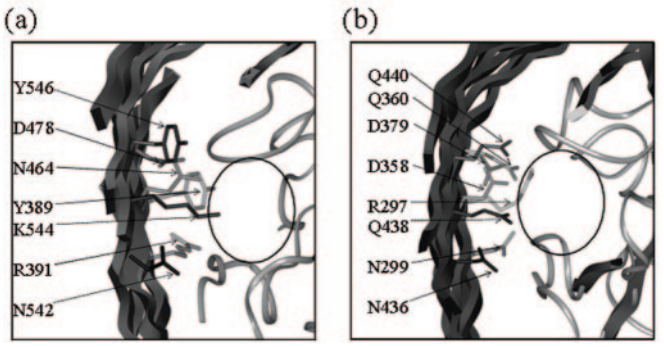

Fig. 5. Location of the channel-forming regions within the 3D TbpA model (**a**) and FhuA–ferrichrome (**b**). Both proteins are viewed from the external surface along the barrel axis. Sections of the β-barrels of TbpA and FhuA are shown as black strands. Plug domains from both proteins are displayed as grey ribbons and channels are circled in black. The side chains of β-barrel residues proposed to border one side of the channel are also displayed and annotated, with the exception of G466 from TbpA.

was assumed that these residues would also be oriented to allow salt-bridge formation. Figure 4 shows that this is the case.

On closer inspection (Figure 5), the model is seen to possess a channel running directly between the external and internal surfaces, located in a similar position to the channel observed in the FhuA–ferrichrome structure. In space-filling versions of the model the channel opening has a diameter of ~8 Å, which then constricts to 5 Å at its narrowest point. Residues lining the TbpA channel are located on the surface of the plug domain and within transmembrane β-strands 7, 8, 9 and 10. Eight β-strand residues postulated to be important for the surface diffusion of ferrichrome through FhuA (Ferguson *et al.*, 1998) are highlighted in the alignment in Figure 2. Two of these residues are conserved in TbpA, while five of the remaining six residues contribute to a hydrophilic environment along the length of the channel that would be required for passage of iron. To check whether this is a general characteristic of TonB dependent proteins, the β-barrel domains of FepA and FecA were superimposed on that of FhuA and the corresponding residues that line the internal channel highlighted. As can be seen from Table II, the majority of these residues are hydrophilic in nature.

Table II. Residues lining the putative internal channel in TonB-dependent proteins

β-Strand	FhuA	FepA	FecA	TbpA
7	R297	S304	N355	Y389
7	N299	W306	Q357	R391
8	D358	H348	E388	N464
8	Q360	D350	R390	G466
9	D379	E368	R409	D478
10	N436	S405	S442	N542
10	Q438	A407	T444	K544
10	Q440	I409	A446	Y546

Discussion

The crystal structures of FepA, FhuA and FecA provide important clues concerning the architecture of all TonB-dependent receptors including TbpA, an important pathogenicity factor in meningococcal disease and a strong candidate for inclusion in a vaccine capable of eliciting protection against all meningococcal serogroups. This study has developed a 3D model of TbpA, using FepA and FhuA as structural templates, that provides a solid basis for further study of the protein. Low sequence identities between TbpA and these templates meant that an accurate model could not be obtained through standard homology modelling techniques alone. However, by taking into account the general hydrophobicity profile displayed by transmembrane β-barrels and characteristics common to the determined structures of siderophore receptors and porins, we believe the validity of the model is sufficient to explain the highly immunogenic nature of TbpA and will allow the mapping of antibodies to surface-exposed, rather than irrelevant, areas of the protein. An important feature of the model in terms of vaccine development is the high degree of surface exposure displayed by the external loops. The longest of these extends up to 60 Å away from the membrane (compared with 35 Å for FhuA), far above the bacterial lipopolysaccharide matrix and presumably more accessible to the host's defence mechanisms than other membrane proteins. This high immunogenic character may explain why antibodies to TbpA are found in the sera of asymptomatic carriers of *N.meningitidis*, in addition to individuals convalescing from meningococcal

disease, and why TbpA antibodies cross-react with a range of meningococcal isolates. The surface exposure of TbpA in the membrane predicts that it would be an important component of an outer membrane vesicle vaccine if its expression could be upregulated, possibly by modification of its promoter sequence. This approach to improve current meningococcal vaccines has been described by Poolman and Berthet (2001).

The TbpA topology model presented includes a putative 158 residue N-terminal plug domain. The 3D model predicts that this sits within a β-barrel of 22 transmembrane strands, a figure indicated not solely by hydropathy profile analysis, but also by the structurally conserved nature of the β-sheet core found within the TbpA plug domain. This suggests that the TbpA β-barrel possesses similar dimensions to that of FepA and is therefore most likely to be 22-stranded. A larger barrel size would diminish the degree of hydrogen bonding between plug domain and barrel wall and reduce conformational stability, whereas a barrel with fewer transmembrane strands would impose a degree of torsional strain on the β-sheet. This feature of the TbpA model is also consistent with the known structures of transmembrane β-barrels – these all contain an even number of up to 22 anti-parallel strands.

The search for hTf-binding epitopes within TbpA has so far been confined to identifying, within the sequence, the external loops in which they reside. One study, based on a 2D topology model of gonococcal TbpA, highlighted three loops, which, when removed by deletion mutagenesis, either abolished hTf binding (loops 4 and 5) or resulted in a 10-fold reduction in ligand binding compared with the wild-type (loop 8) (Boulton *et al*., 2000). In the model presented here, external loops 4 and 5 each possess two positively charged, surface-exposed residues. Loop 8 contains two lysines (K677 and K684), an aspartate (D678) and two glutamates (E681 and E682) in a tight cluster at the apex of the loop. The side chains of all these are highly exposed to the environment which, in conjunction with the results of the deletion study, suggests that they play a role in initial binding events with hTF. Such observations are not possible from topology predictions alone, hence the 3D model represents a significant advance in allowing a targeted approach to site-directed mutagenesis studies and antibody generation. The identification of ligand binding motifs is currently the aim of ongoing studies using the established expression system for producing purified, recombinant TbpA (Oakhill *et al*., 2002). The 3D model also suggests the possibility for disulphide bond formation between cysteine pairs in loops 2, 4 and 5. Since the short external loop regions between these cysteine pairs are surface exposed to a large degree, the more rigid tertiary structure imparted upon them by the disulphide bond could be important for hTF binding and/or protein function. Such a feature may be particularly significant for loop 4, in which the region bordered by disulphide bond-forming cysteine residues extends directly into the cavity lying between the external apex of the plug domain and the putative hTF binding cleft. This raises the possibility of synthetically producing, or independently expressing, peptides corresponding to these three regions, in which the disulphide bond would promote formation of the native fold. The peptides can be used to raise antibodies that are predicted, with some confidence from the TbpA model, to bind to the external surface of TbpA and physically disrupt hTF binding.

The model possesses characteristics that may be relevant to the mechanism of iron translocation employed by TbpA, although inferences made at this stage must be treated with caution. Access to the external surface of the plug domain is restricted to a cleft no wider than 15 Å in diameter. Although the model is a static representation of the receptor located within a fluid membrane and the external loops presumably possess a degree of flexibility, it is still difficult to envisage how a molecule as large as hTf could be brought into close enough contact with sites deep within the TbpA binding pocket to allow ferric iron transfer. However, the finding from the mutagenesis study that loops 4 and 8 of gonococcal TbpA may contain hTf-binding motifs lends support to the theory that iron release from hTf is facilitated by a multi-determinant binding stage involving several external loops of TbpA, followed by conformational rearrangements to expose the iron-binding site of hTf. Within the model presented here, external loops 4 and 8 are located on either side of the cleft leading to the plug domain and, once docked to adjacent domains on hTf and perhaps in conjunction with TbpB, would be favourably positioned to provide the force required to separate them. Therefore, a principal function of TbpA's long external loops may be to aid in the active removal of iron from hTf.

The conformational changes seen in the shorter external loops of FecA–diferricitrate complex appear to be directed at retaining the ligand in the binding pocket prior to translocation and to prevent the indiscriminate flow of solutes through an open pore. Any differences in the roles of the external loops of TbpA and FecA will suggest that the receptors have evolved to overcome the specific problems associated with their ligand. It is possible that TbpA has no need to employ a gating mechanism, since the interaction with hTF, involving a contribution from the other long external loops and/or TbpB, may be sufficient to seal the entrance to the TbpA pore from the extracellular space. The 3D TbpA model also reveals a channel running right through the molecule, lined by predominantly hydrophilic residues located on the interior of the barrel wall. These features are also evident in the structure of the FhuA–ferrichrome complex. The charge distribution at either end of the TbpA channel is also similar to that found in FhuA, with an aspartate residue located at the external entrance and an arginine residue located at the periplasmic end. Residues on the interior surface of the FhuA barrel that border on to this channel are proposed to act as low-affinity binding sites for ferrichrome iron, which would be passed from site to site during its passage through the membrane. Such a mechanism has been proposed to occur in the translocation of maltodextrins through channels in the protein LamB (Schirmer *et al*., 1995). Given that these residues are found in four different transmembrane strands, their structural and positional conservation between TbpA and FhuA is all the more significant. However, the inability to position water molecules accurately within the model is a limitation of this study and provides no clues as to whether ejection of the plug from the barrel during iron transport is energetically possible. The degree of solvation that exists at the interface between the two TbpA domains will only become evident with the determination of an atomic structure. However, it seems likely that at some point in the process, prior to iron entering the channel, the mechanisms employed by TbpA and the siderophore receptors converge, after which iron transport occurs via a common pathway.

Acknowledgements

J.S.O. was funded by an MRC Collaborative Studentship. Research at Health Protection Agency, Porton Down, was funded by the UK Department of Health.

References

Blanton,K.J., Biswas,G.D., Tsai,J., Adams,J., Dyer,D.W., Davis,S.M., Koch,G.G., Sen,P.K. and Sparling,P.F. (1990) *J. Bacteriol.*, **172**, 5225–5235.
Boulton,I.C., Gorringe,A.R., Shergill,J.K., Joannou,C.L. and Evans,R.W. (1999) *J. Theor. Biol.*, **198**, 497–505.
Boulton,I.C., Yost,M.K., Anderson,J.E. and Cornelissen,C.N. (2000) *Infect. Immun.*, **68**, 6988–6996.
Bradbeer,C. (1993) *J. Bacteriol.*, **128**, 3146–3150.
Brooks,B.R., Bruccoleri,B.D., Olafson,B.D., States,D.J., Swaminathan,S. and Karplus,M. (1983) *J. Comput. Chem.*, **4**, 187–217.
Buchanan,S.K., Smith,B.S., Venkatramani,L., Xia,D., Esser,L., Palnitkar,M., Chakraborty,R., van Der Helm,D. and Deisenhofer,J. (1999) *Nat. Struct. Biol.*, **6**, 56–63.
Cowan,S.W., Schirmer,T., Rummel,G., Steiert,M., Ghosh,R., Pauptit,R.A., Jansonius,J.N. and Rosenbusch,J.P. (1992) *Nature*, **358**, 727–733.
Eisenberg,D., Weiss,R.M. and Terwilliger,T.C. (1984) *Proc. Natl Acad. Sci. USA*, **81**, 140–144.
Faraldo-Gómez,J.D. and Sansom,M.S. (2003) *Nat. Rev. Mol. Cell. Biol.*, **2**, 105–116.
Ferguson,A.D., Hoffman,E., CoultonJ.W., Diederichs,K. and Welte,W. (1998) *Science*, **22**, 2215–2220.
Ferguson,A.D., Chakraborty,R., Smith,B.S., Esser,L., van der Helm,D. and Deisenhofer,J. (2002) *Science*, **295**, 1715–1719.
Freedman,S.J., Blostein,M.D., Baleja,J.D., Jacobs,M., Furie,B.C. and Furie,B. (1996) *J. Biol. Chem.*, **271**, 16227–16236.
Gerlach,G.F., Klashinsky,S., Anderson,C., Potter,A.A. and Wilson,P.J. (1992) *Infect. Immun.*, **60**, 3253–3261.
Gorringe,A.R., Borrow,R., Fox,A.J. and Robinson,A. (1995) *Vaccine*, **13**, 1207–1212.
Gorringe,A.R. and Oakhill,J.S. (2002) In Ferreiròs,C., Criado,M.T. and Vázquez,J. (eds), *Emerging Strategies in the Fight Against Meningitis: Molecular and Cellular Aspects*. Horizon Scientific Press, Wymondham, UK, pp. 119–134.
Greer,J. (1990) *Proteins*, **7**, 317–314.
Griffiths,E. and Williams,P. (1999) In Bullen,J.J. and Griffiths,E. (eds), *Iron and Infection: Molecular, Physiological and Clinical Aspects*. Wiley, Chichester, pp. 87–212.
Johnson,A.S., Gorringe,A.R., Fox,A.J., Borrow,R. and Robinson,A. (1997) *FEMS Immunol. Med. Microbiol.*, **19**, 159–167.
Kamata,K., Kawamoto,H., Honma,T., Iwama,T. and Kim,S.H. (1998) *Proc. Natl Acad. Sci. USA*, **95**, 6630–6635.
Kelley,L.A., MacCullum,R.M. and Sternberg,M.J. (2000) *J. Mol. Biol.*, **299**, 499–520.
Krezel,A.M., Wagner,G., Seymour-Ulmer,J. and Lazarus,R.A. (1994) *Science*, **264**, 1944–1947.
Laskowski,R.A., Moss,D.S. and Thornton,J.M. (1993) *J. Mol. Biol.*, **231**, 1049–1067.
Locher,K.P., Rees,B., Koebnik,R., Mitschler,A., Moulinier,L., Rosenbusch,J.P. and Moras,D. (1998) *Cell*, **95**, 771–778.
Meyer,J.E., Hofnung,M. and Schulz,G.E. (1997) *J. Mol. Biol.*, **266**, 761–775.
Morellet,N., Demene,H., Teilleux,V., Huynh-Dinh,T., De Rocquigny,H., Fournie-Zaluski,M.-C. and Roques,B.P. (1998) *J. Mol. Biol.,* **283**, 419–434.
Neuhaus,D., Nakaseko,Y., Schwabe,J.W. and Klug,A. (1992) *J. Mol. Biol.*, **228**, 637–651.
Oakhill,J.S., Joannou,C.L., Buchanan,S.K., Gorringe,A.R. and Evans,R.W. (2002) *Biochem. J.*, **364**, 613–616.
Pajón,R., Chinea,G., Marrero,E., Gonzalez,D. and Guillen,G. (1997) *Microb. Pathog.*, **23**, 71–84.
Poolman,J. and Berthet,F.X. (2001) *Vaccine*, **20**, Suppl 1, S24–S26.
Sali,A. and Blundell,T.L. (1993) *J. Mol. Biol.*, **234**, 779–815.
Schirmer,T. and Cowan,S.W. (1993) *Protein Sci.*, **2**, 1361–1363.
Schirmer,T., Keller,T.A., Wang,Y.F. and Rosenbusch,J.P. (1995) *Science*, **267**, 512–514.
Schryvers,A.B. and Lee,B.C. (1989) *Can. J. Microbiol.*, **35**, 409–415.
Schryvers,A.B. and Stojiljkovic,I. (1999) *Mol. Microbiol.*, **32**, 1117–1123.
Sticht,H., Pickford,A.R., Potts,J.R. and Campbell,I.D. (1998) *J. Mol. Biol.*, **276**, 177–187.
Torres,A.M. *et al*. (1999) *Biochem. J.*, **341**, 785–794.
Usher,K.C., Ozkan,E., Gardner,K.H. and Deisenhofer,J. (2001) *Proc. Natl Acad. Sci. USA*, **98**, 10676–10681.
Weiss,M.S., Kreusch,A., Schiltz,E., Nestel,U., Welte,W., Weckesser,J. and Schulz,G.E. (1991) *FEBS Lett.*, **280**, 379–382.
West,D., Reddin,K., Matheson,M., Heath,R., Funnell,S., Hudson,M., Robinson,A. and Gorringe,A.R. (2001) *Infect. Immun.*, **69**, 1561–1567.

Received November 11, 2004; revised March 16, 2005; accepted March 19, 2005

Edited by Hagan Bayley